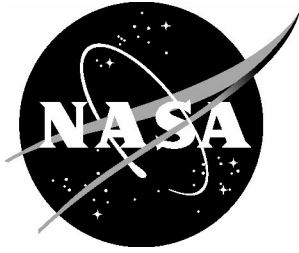


NASA/TM-2015-43: 99:



Comparison of Analysis with Test for Static Loading of Two Hypersonic Inflatable Aerodynamic Decelerator Concepts

*Karen H. Lyle
Langley Research Center, Hampton, Virginia*

NASA STI Program . . . in Profile

Since its founding, NASA has been dedicated to the advancement of aeronautics and space science. The NASA scientific and technical information (STI) program plays a key part in helping NASA maintain this important role.

The NASA STI program operates under the auspices of the Agency Chief Information Officer. It collects, organizes, provides for archiving, and disseminates NASA's STI. The NASA STI program provides access to the NTRS Registered and its public interface, the NASA Technical Reports Server, thus providing one of the largest collections of aeronautical and space science STI in the world. Results are published in both non-NASA channels and by NASA in the NASA STI Report Series, which includes the following report types:

- **TECHNICAL PUBLICATION.** Reports of completed research or a major significant phase of research that present the results of NASA Programs and include extensive data or theoretical analysis. Includes compilations of significant scientific and technical data and information deemed to be of continuing reference value. NASA counter-part of peer-reviewed formal professional papers but has less stringent limitations on manuscript length and extent of graphic presentations.
- **TECHNICAL MEMORANDUM.** Scientific and technical findings that are preliminary or of specialized interest, e.g., quick release reports, working papers, and bibliographies that contain minimal annotation. Does not contain extensive analysis.
- **CONTRACTOR REPORT.** Scientific and technical findings by NASA-sponsored contractors and grantees.

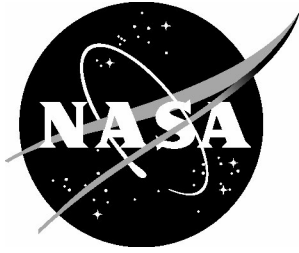
- **CONFERENCE PUBLICATION.** Collected papers from scientific and technical conferences, symposia, seminars, or other meetings sponsored or co-sponsored by NASA.
- **SPECIAL PUBLICATION.** Scientific, technical, or historical information from NASA programs, projects, and missions, often concerned with subjects having substantial public interest.
- **TECHNICAL TRANSLATION.** English-language translations of foreign scientific and technical material pertinent to NASA's mission.

Specialized services also include organizing and publishing research results, distributing specialized research announcements and feeds, providing information desk and personal search support, and enabling data exchange services.

For more information about the NASA STI program, see the following:

- Access the NASA STI program home page at <http://www.sti.nasa.gov>
- E-mail your question to help@sti.nasa.gov
- Phone the NASA STI Information Desk at 757-864-9658
- Write to:
NASA STI Information Desk
Mail Stop 148
NASA Langley Research Center
Hampton, VA 23681-2199

NASA/TM-2015-43: 99:



Comparison of Analysis with Test for Static Loading of Two Hypersonic Inflatable Aerodynamic Decelerator Concepts

*Karen H. Lyle
Langley Research Center, Hampton, Virginia*

National Aeronautics and
Space Administration

Langley Research Center
Hampton, Virginia 23681-2199

June 2015

The use of trademarks or names of manufacturers in this report is for accurate reporting and does not constitute an official endorsement, either expressed or implied, of such products or manufacturers by the National Aeronautics and Space Administration.

Available from:

NASA STI Program / Mail Stop 148
NASA Langley Research Center
Hampton, VA 23681-2199
Fax: 757-864-6500

Abstract

Acceptance of new spacecraft structural architectures and concepts requires validated design methods to minimize the expense involved with technology demonstration via flight-testing. Hypersonic Inflatable Aerodynamic Decelerator (HIAD) architectures are attractive for spacecraft deceleration because they are lightweight, store compactly, and utilize the atmosphere to decelerate a spacecraft during entry. However, designers are hesitant to include these inflatable approaches for large payloads or spacecraft because of the lack of flight validation. This publication summarizes results comparing analytical results with test data for two concepts subjected to representative entry, static loading. The level of agreement and ability to predict the load distribution is considered sufficient to enable analytical predictions to be used in the design process.

Introduction

High reliability entry, descent, and landing systems have been in demand for all classes of space applications. Specific applications include International Space Station (ISS) return mass, sample return, Mars exploration vehicles, and human-rated exploration vehicles. Architectures that incorporate Hypersonic Inflatable Aerodynamic Decelerators (HIADs) show promise for many of these applications, as discussed in Refs. [1-3]. Also various Inflatable Aerodynamic Decelerators (IADs) were proposed, studied, and reported in publications dating from the 1960s, see Refs. [4-6]. More recently, a series of small-scale test flights have demonstrated a basic functionality of a stacked torus configuration at the 3-m diameter scale, see Refs. [7 and 8]. HIAD diameters up to 81-m have been proposed, Ref. [1]. Traditionally, for such designs to gain acceptability, they need to be verified and validated through full-scale testing. Unfortunately, ground test demonstration of the structural reliability to aerodynamic loading is difficult due to limited test facility size and gravity effects. Therefore, such concepts will require certification through test-validated analysis. Fortunately, significant advances have occurred in the numerical simulation of these complex structural systems. For example, simulations can incorporate structural aspects such as geometrically accurate models and advanced material models to include nonlinear stress-strain behaviors, woven fabrics, and airbag inflation. This was demonstrated for the Orion Landing System – Advanced Development Project, where the spacecraft landing system effectively incorporated modeling of airbags (soft goods) in the early design process, see Refs. [9 and 10]. Additional simulations incorporating structural members with fabrics can be found in Refs. [11 and 12].

For this HIAD family of structures, a series of stacked tori are constrained by a network of woven straps. The HIAD structural analysis problem presents several design challenges: 1) Formal design approaches do not exist to address the various HIAD concepts. 2) HIAD structures exhibit complex structural responses to include soft goods and numerous load paths. 3) Such systems require computationally efficient and robust modeling tools to support the design and development phases. Detailed computational tools to analyze the structural response of such systems are becoming sufficiently mature to accurately model the response of these complex structures. Computationally efficient models are also critical to enable completion of hundreds of transient dynamics simulations needed to verify the design.

A previously published document, Ref. [13], contains a description of the global sensitivity analysis results that focused on the impact of material parameters (such as the elastic modulus and the fabric weave angle) on the deformed shape and cone angle. In that study, the parameters were allowed to vary by as much as a factor of 10 and results showed that the elastic modulus of the straps and tori dominated the uncertainty.

To contrast, the work here concentrates on providing initial comparisons of analysis results with test data for various loading conditions. Specifically, models for two concepts (designated Concept A and Concept B in this report) will be compared with the test data. Following testing of Concept A in 2012, modifications were made to the structure to reduce weight while improving performance. Subsequently, Concept B was tested in 2014. A brief description of the static testing is followed by a description of the finite element models (FEMs). The results focus on HIAD shape under loading and the loads in the straps. Concluding remarks provide general comments about adequacy of the model and simulations to support design studies.

Test Description

A HIAD concept in the static test facility with the forward side facing up is shown in Figure 1(a). The tori are numbered from innermost outward. Thus, the small torus bearing against the Center Body is designated Torus 1 and the outermost torus is Torus 8. Straps are arranged to ensure that loads are reacted through the Center Body. The tori and straps are initially all separate parts. The final inflatable structure is constructed by adding tori and straps one-at-a-time from the Center Body outward. The numerous straps are tightened individually to achieve the desired initial shape. Once the straps and tori initial locations are in place, room temperature vulcanization (RTV) silicone was used to “fix” the torus-to-torus and torus-to-strap interference bonds. In general, these bonds held during the testing.

A thin flexible cover is placed over the forward side of the HIAD and sealed at the junction with the vacuum tub, as shown in Figure 1(b). A vacuum is then applied to the aft side of the HIAD to mimic the static pressure differential that is experienced by the structure during the hypersonic deceleration phase of atmospheric entry. This cover pressure load is designated p_v . Additional details of this test program as well as related elemental and component testing can be found in Refs. [14 and 15].

Over the period of three years from 2012 to 2014, a number of full-scale inflatable structures were exposed to static loads expected during a mission. During these test series, the axial displacement of Torus 7 was measured as well as the loads in various straps. Ultimately, aerodynamic performance is dependent on the forward shape of the HIAD. The cone angle, approximated by the coordinates of Torus 1 and Torus 7, was used to represent the global shape. The tori coordinates, computed from the displacements, provide a direct measurement of the deformed shape as a function of an applied aerodynamics load. Knowledge of the deformed shape would be used to conduct predictions of the aerodynamic stability, heating loads, and control performance during re-entry. Knowledge of the strap loads is important to assess load distribution and sizing of the straps for the expected loads.

Model Description

The numerical simulations were executed in LS-Dyna™, a commercial, general-purpose, nonlinear, transient-dynamic, finite element code, see Ref. [16]. A baseline (or as-delivered) model, was provided by the HIAD vendor and modified to correspond to the as-tested tori and strap configurations, strap and axial cord material properties, material thicknesses, and contact definition details.

Figures 2 and 3 show the FEM representations for Concept A and Concept B, respectively. In the figures, the radial and chevron straps are represented in black, the pairing loop straps in gray, the tori in alternating gold and rose, the center body in green, and the axial cords in pink. For both concepts, the complete FEM is provided in (a). Many of the radial straps are often co-incident, but not attached, to the pairing loop straps. This co-incident leads to software visualization issues at many of the strap locations. Therefore, separate figures highlighting the pairing loop straps (b) and radial and chevron straps (c) have been included. Comparing Figures 2(c) and 3(c), it is apparent that the radial to Torus 5 and the chevron to Torus 7 have been removed for Concept B. An additional torus (designated Torus 5.5) was incorporated in Concept B, see Figure 4. To accommodate the addition of Torus 5.5, the pairing loop straps holding Torus 5 and Torus 6 together in Concept A have been expanded.

A number of unique modeling features were implemented in the simulations. For example, the tori and straps are represented as fabric material models. This fabric model was originally developed for automotive airbag applications. Specifically, the fabric material model is based on an existing orthotropic composite model only valid for membrane elements. However, this material model has since been used in broader applications as documented in Refs. [11 and 12]. The axial cords are represented as 2-D seatbelt elements and assigned seatbelt material properties, which allow the user to input nonlinear loading and unloading load-strain curves. Like the tested HIAD axial cords, these specialized seatbelt elements do not allow compressive loads. The center body is assigned rigid material properties. The tori are inflated using the Wang-Nefske airbag model. The FEMs for Concepts A and B contained over 250,000 nodes, 220,000 4-node, fully-integrated, shell elements and 3500 2-node seatbelt elements.

A critical aspect for successful shape prediction for this application is an appropriate sequence of events at the beginning of the simulations. This sequence directly impacts the initial tori inflations, strap loads, and interference bonds (also designated “contact” in LS-Dyna™). Contact is a numerical modeling technique used in these types of applications to prevent the penetration of one part into another and allow two non-connected parts to interact with forces. Details about the implementation of contact modeling can be found in *LS-Dyna User's Manual*, Ref. [16]. In our simulations, the event sequence has been divided into four steps.

Step 1) The simulations begin with tori-to-tori positions showing some interference, see Figure 5(a), since no contacts have been defined. For clarity, a wedge of the complete model with straps removed has been extracted. The tori and straps have been sized and positioned in the model to mimic the test article. This overlap at the outset will enable the tori to effectively bear against each other by the end of Step 3. At the start of the simulations, the tori pressures are prescribed based on test data. For Concept A, the tori

pressures are set to the final inflated state. A number of tori pressure combinations (p_t) were tested experimentally, see Table 1. For Concept B, all of the tori are initially inflated to 2 psi for this step.

Step 2) The tori are then compressed by applying a pressure to the external surface of each torus to uniformly reduce the diameter, see Figure 5(b). This pressure applied to the external surface must be greater than the internal pressure specified in Step 1 to produce the desired results. Once the tori are compressed to the point where no interference is evident, the contact definitions are enabled.

Step 3) The tori external compression loads are now ramped down to zero, which allows the tori to expand under the internal pressure prescribed in Step 1. Since the contact has been enabled, as the tori expand then the torus-to-torus and torus-to-strap contacts are effective, see Figure 5(c). Note that the interference between tori in Figure 5(a) has been eliminated. For Concept B only, the tori are now inflated to the test values by applying an additional 13-psi pressure load to the internal surfaces of the tori. At the end of Step 3, the HIAD cover is ready to be loaded.

Step 4) A pressure load (equal to the vacuum pressure) is applied to the forward (top) side of the cover. The final shape of the HIAD structure is shown in Figure 5(d). The cover load produces an overall decrease in the cone angle and an aft-ward deflection of Torus 7. Additional details, specific to each concept, are provided.

- In Concept A, the cover pressure is ramped up to the final value over 0.02 seconds; and the contact frictions are set to 0.5, which is sufficient to keep the various parts fixed relative to each other. The transient solution is allowed to run for 0.2 seconds at which time the transient dynamics are insignificant. All results are extracted at 0.2 seconds. Thus, for each of the cover pressure load cases, a separate simulation is required. These simulations required 4 hours on 4 CPUs for each load condition using double precision.
- For Concept B, the maximum cover pressure load is slowly ramped up over 8 seconds, which more closely simulates the quasi-static test loading. The slower loading mitigates the transient response and allows for the extraction of intermediate loading conditions during one simulation. The contact friction is increased to 3.0 to prevent the relative motion of the torus-to-torus and torus-to-strap bonds. Note that these contact friction values are simply a numerical method to “bond” the parts. Concept B simulations required 3 days on 4 CPUs using double precision.

Results

The photograph of Concept A under vacuum load in the test facility, see Figure 6(a), shows the conforming of the cover to the HIAD structure. The indentations of the straps on the tori are also visible. Similarly, the FEM model, with an equivalent pressure load applied to the forward side of the cover, shows significant conforming of the cover and the indentations of the straps into the tori, see Figure 6(b).

Early model assessments were based on comparisons of the center body loads and the load distribution in the straps. Significant uncertainty existed in the measured strap load distribution at inflation (Step 3) due to uncertainty in the unloaded strap lengths. Therefore, the project requested that all strap load results (measured and predicted) be presented relative to the state at the end of Step 3. A comparison of global loads for the

case where all tori are inflated to $p_t = 15 \text{ psi}$ and the cover load is $p_v = 0.75 \text{ psi}$, results in 28,364 lb for the test and 27,855 lb for the analysis. Note that the analytical predictions of the global load are within 2% of the measured values. To contrast, loads at individual straps are shown in Figure 7, for both test and analysis. The design loads for these straps range from 2,000 to 4,000 lb. Thus, except for the radial straps near the center body, the strap loads are well below the limits. The nonlinearity of the strap load behavior for relatively low loads may also account for some of the large differences when examined as a percentage. The predicted strap loads are dependent on the relative locations of the straps and tori as the tori compressive loads are released. The test strap loads are dependent on the hand lay-up of the straps as the HIAD structure is constructed. When comparing test to analysis, the error in the strap loads ranged from under 2% to as much as 42%. Thus, the LS-DYNA model is able to predict well global loads, but predictive capability of the detailed strap loads is mixed. The significance of the errors in the strap loads at these low design loads has yet to be determined. Visually presenting data in the format provided in Figure 7 makes it difficult to assess overall model adequacy for multiple load/inflation combination cases.

Henceforth, the strap load results for several test pressures (p_t and p_v) are consolidated on one chart. In Figure 8 for Concept A, the predicted values are presented along the abscissa and the test values on the ordinate. A total of 31 out of 32 load values fall within the dashed lines that indicate the $\pm 100 \text{ lbs}$ bounds. Note that data for all locations shown in Figure 7 were not available for all load conditions. In particular, for both the $p_t = 15/10 \text{ psi}$ and $p_t = 15/12.5 \text{ psi}$ cases, data for only 3 strap locations were available. Readers should know that some of the test data are averages for multiple "axisymmetric" locations, while others are response values from a single measurement. It is also important to note that some circumferential asymmetry was observed experimentally and reported in Ref. [15]. To assess strap load variations for Concept A for the entire surface, Table 2 shows: the mean errors of the strap loads, $(\text{Test-Pred})_{\text{mean}}$; and the mean of the error magnitudes $|\text{Test-Pred}|_{\text{mean}}$.

Another important assessment metric for the system is the angle a line tangent to the tori surface makes with respect to the central body. This angle, referred to as the coning angle, is used as a measure of surface quality. Figure 9 shows the Concept A coning angle which is computed as the slope of the radial versus axial position. The test and prediction coning angles have been provided in Table 3 to provide a quantifiable metric. These results show that if the preliminary design goal was to predict the coning angle to within 0.5 degrees, then the current model satisfies the requirement. Specifically, the observed small cone angle variations between test and analysis are not considered to be significant enough to impact the aerodynamic performance.

Two interim observations can be made as a result of processing the test and prediction data for Concept A. 1) For multiple tori inflation and cover loading conditions, an acceptable level of agreement in the cone angle and global loads between test and analysis is shown. Of the five load cases studied for Concept A, four are for differing tori inflation combinations p_t , but the same cover load $p_v = 0.55 \text{ psi}$. 2) The complex loading sequence related to tori inflation, compression, contact initiation and cover loading are adequately modeled using LS-Dyna™.

Two major issues were identified for additional work. First, the adequacy of the contact method to model the test article interference bonds was assessed. Specifically, a

number of numerical studies were performed to evaluate sensitivity of the predicted results to the contact friction modeling. These studies resulted in an increase in contact friction to adequately “fix” the relative motion of the various parts under a more challenging load condition. Second, the impact on the dynamic behavior of the cover-pressure loading rate (Step 4) was evaluated. For Concept A, the loading rate was quick to shorten runtime. A reduced ramping rate of the cover load was exercised in Concept B to mitigate the dynamic effects.

The next two figures provide results for subsequent simulations implementing the changes highlighted above. A companion set of results for Concept B strap loads have been processed and consolidated on one chart, see Figure 10 and one table, see Table 4. In this case, the tori inflation conditions are held constant, while the cover load is varied. Figure 10 shows analysis and test results for all the strap loads measured and predicted as well as the +/- 100 lbs bounds. In this case, 34 out of 42 strap load values are within the desired bounds. Table 4 shows the mean error metrics. As the pressure load increases, the absolute value of the difference increases and shows a nearly linear relationship with cover pressure. Unlike Concept A, the test cone angle is greater than or equal to the prediction values, see Figure 11 and Table 5. Again, these differences are well within the proposed 0.5-deg. requirement and will not impact the aerodynamic performance.

Finally, the relative adequacy of the two modeling approaches (Concept A and Concept B) was also evaluated. Based on these comparisons, the difference in cover loading rate did not appreciably impact the prediction errors. The selection of loading rate is likely dependent on the number of cover loading states to be examined and the available computation time. However, care must be exercised in selection of contact friction to prevent slipping of parts.

Concluding Remarks

Data from multiple ground tests of a 6m-HIAD inflatable structure have been used to compare simulation results with test. The finite element model used for comparison is a revised version of the contractor delivered model. Model revisions include updated material properties, updated test conditions, and minimal modifications to the complex simulation sequence of events. One of the main goals for the study was to develop confidence in this type of analysis code to predict the structural response of an inflatable structure under a representative reentry aerodynamic load. For this type of reentry vehicle, aerodynamic performance relies heavily on the forward shape (i.e., cone angle) under load. From this study, it was determined that predicted cone angles were within 0.5-degrees of the measured values, which satisfied the requirements. Additionally strap loads, a major design concern, were predicted at various locations. The vast majority of the individual strap loads were predicted to be within 100 lbs of the measured loads. In addition, the mean errors of the straps loads were well within the 100-lb bounds. Hence, this level of agreement of the cone angle and the strap loads is considered sufficient to enable these types of analysis tools to be used in the design process.

Acknowledgement

The author would like to acknowledge Mr. Benjamin Tutt (Airborne Systems North America) for generating the baseline HIAD LS-Dyna model. The vendor-provided model

incorporated several unique modeling features and overall replicated the physics of the testing quite well.

References

1. Dwyer Cianciolo, A. M., *et al*: Entry, Descent and Landing Systems Analysis Study: Phase 1 Report. NASA TM 2010-216720, July 2010.
2. Smith, B. P., *et al*: A Historical Review of Inflatable Aerodynamic Decelerator Technology Development. Proceedings of the 2010 IEEE Aerospace Conference, IEEEAC Paper No. 1276, Big Sky MT, March 2010.
3. Bose, D. M., *et al*.: The Hypersonic Inflatable Aerodynamic Decelerator (HIAD) Mission Applications Study. Proceedings of the AIAA Aerodynamic Decelerator Systems Conference, AIAA Paper No. 2013-1389, Dayton Beach FL, March 25-28, 2013.
4. Leonard, R. W.; Brooks, G. W.; McComb, H. G.: Structural Considerations of Inflatable Reentry Vehicles. NASA TND-457, September 1960.
5. Anderson, J. S.; Robinson, J. C.; Bush, H. G.; Fralich, R. W.: A Tension Shell Structure for Application to Entry Vehicles, NASA TN D-2675, March 1965.
6. Bohon, H. L.; and Miserentino, R.: Attached Inflatable Decelerator Performance Evaluation and Mission-Application Study. Proceedings of the AIAA Aerodynamic Deceleration Systems Conference, AIAA Paper No. 70-1163, Dayton OH, September 14-16, 1970.
7. Lindell, M. C.; Hughes, S. J.; Dixon, M. and Willey, C. E.: Structural Analysis and Testing of the Inflatable Re-entry Vehicle Experiment (IRVE). Proceedings of the 47th AIAA/ASME/ASCE/AHS/ASC Structures, Structural Dynamics, and Materials Conference, AIAA Paper No. 2006-1699, Newport RI, May 1-4, 2006.
8. Hughes, S. J., *et al*.: Inflatable Re-entry Vehicle Experiment (IRVE) Design Overview. Proceedings of the 18th AIAA Aerodynamic Decelerator Systems Technology Conference and Seminar, AIAA Paper AIAA 2005-1636, Munich, Germany, May 23-26, 2005.
9. Timmers, R. B.; Hardy, R. C.; and Welch, J. V.: Modeling and Simulation of the Second-Generation Orion Crew Module Air Bag Landing System. Proceeding of the 20th AIAA Aerodynamic Decelerator Systems Technology Conference and Seminar, AIAA Paper No. 2009-2921, Seattle WA, May 4-7, 2009.
10. Tutt, B.; Johnson, R. K.; and Lyle, K.: Development of an Airbag Landing System for the Orion Crew Module. Proceedings of the 10th International LS-Dyna Users Conference, Dearborn MI, June 8-10, 2008.
11. Tutt, B. A.; and Taylor, A. P.: Applications of LS-Dyna to Structural Problems Related to Recovery Systems and Other Fabric Structures. Proceedings of the 7th International LS-Dyna Users Conference, Dearborn MI, May 19-21, 2002.
12. Tanner, C. L.; Cruz, J. R.; Braun, R. D.: Structural Verification and Modeling of a Tension Cone Inflatable Aerodynamic Decelerator. Proceedings of the 51st AIAA/ASME/ASCE/AHS/ASC Structures, Structural Dynamics, and Materials Conference, AIAA Paper No. 2010-2830, Orlando FL, April 12-15, 2010.
13. Lyle, K. H.: Preliminary Structural Sensitivity Study of Hypersonic Inflatable Aerodynamic Decelerator Using Probabilistic Methods. NASA TM-2014-218290, July 2014.
14. Cassell, A. M., *et al*: Overview of Hypersonic Inflatable Aerodynamics Decelerator Large Article Ground Test Campaign. Proceedings of the 21st AIAA Aerodynamic Decelerator Systems Technology Conference and Seminar. AIAA Paper No. 2011-2569, Dublin, Ireland, May 23-26, 2011.

15. Swanson, G. T., *et al*: Structural Strap Tension Measurements of a 6 meter Hypersonic Inflatable Aerodynamic Decelerator under Static and Dynamic Loading. Proceedings of the AIAA Aerodynamic Decelerator Systems Conference, AIAA Paper No. 2013-1287, Dayton Beach FL, March 25-28, 2013.
16. *LS-Dyna Keyword User's Manual*, Version 971, July 27, 2012 (revision: 1617).

Table 1. Concept A tori pressure conditions

p_t, psi	Torus Pressures, psi	
	1-2	3 - 8
20	20	20
15	15	15
15/10	15	10
15/12.5	15	12.5

Table 2. Concept A strap load mean errors.

p_t, psi	p_v, psi	(Test-Pred)_{mean}, lb	 Test-Pred _{mean}, lb
20	0.55	17	55
15	0.55	-4	22
15	0.75	-8	37
15/10	0.55	26	41
15/12.5	0.55	-7	27

Table 3. Concept A cone angle.

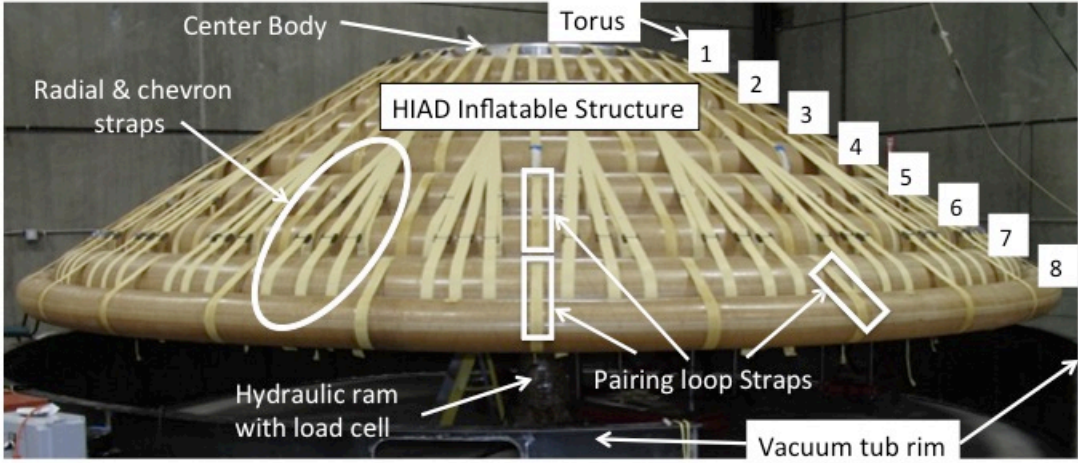
p_t, psi	p_v, psi	Test, deg.	Pred, deg.
20	0.55	58.8	58.8
15	0.55	58.4	58.5
15	0.75	57.8	58.1
15/10	0.55	57.6	58.2
15/12.5	0.55	58.3	58.6

Table 4. Concept B strap load mean errors.

p_t, psi	p_v, psi	(Test-Pred)_{mean}, lb	 Test-Pred _{mean}, lb
15	0.25	-6	30
15	0.50	-11	58
15	0.75	-15	79

Table 5. Concept B cone angles.

p_t, psi	p_v, psi	Test, deg.	Pred, deg.
15	0.25	58.9	58.6
15	0.50	58.4	58.0
15	0.75	57.9	57.5



(a) Concept A test article – Without cover



(b) Concept A test article – With cover

Figure 1. HIAD in Test Facility

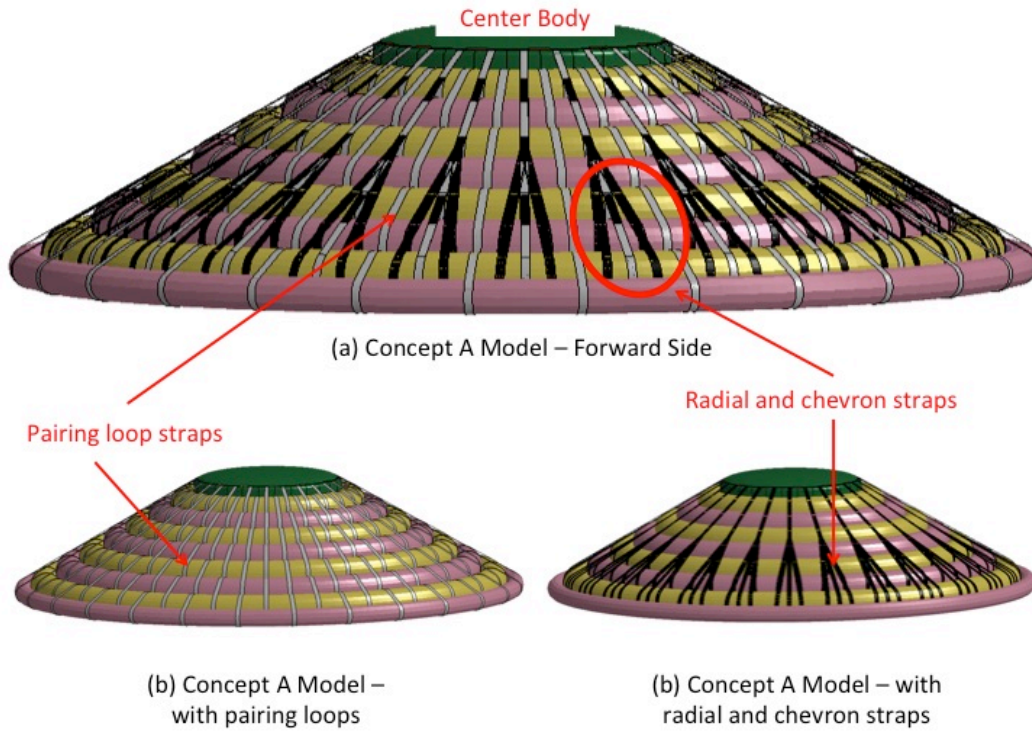


Figure 2. FEM of Concept A.

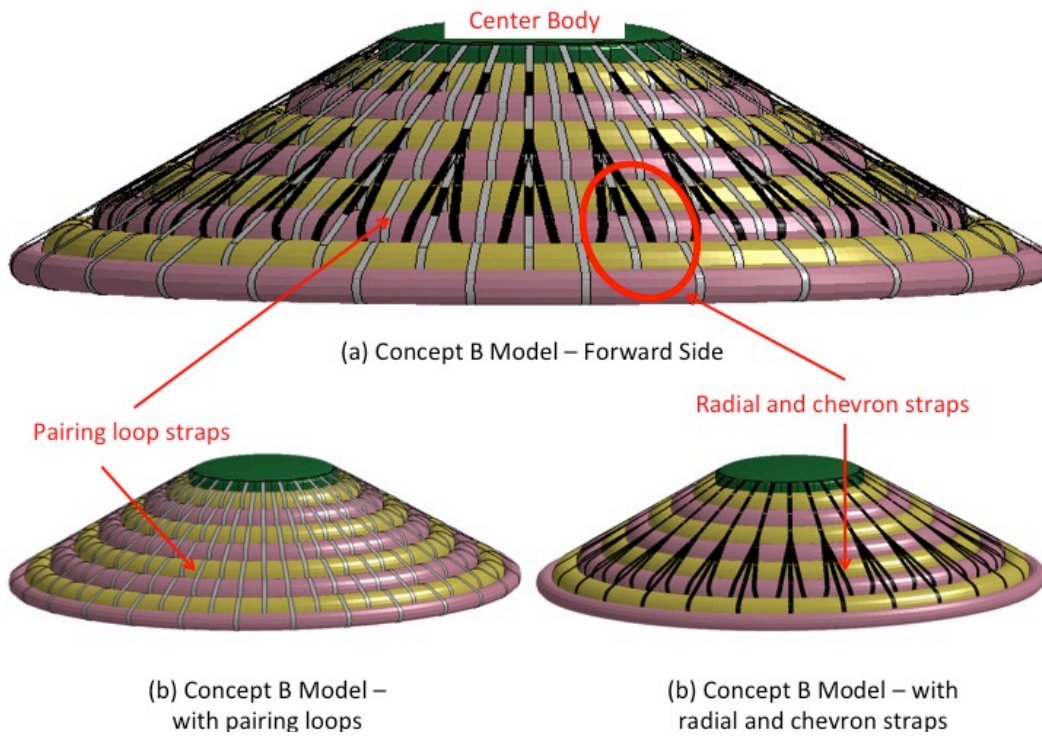


Figure 3. FEM of Concept B.

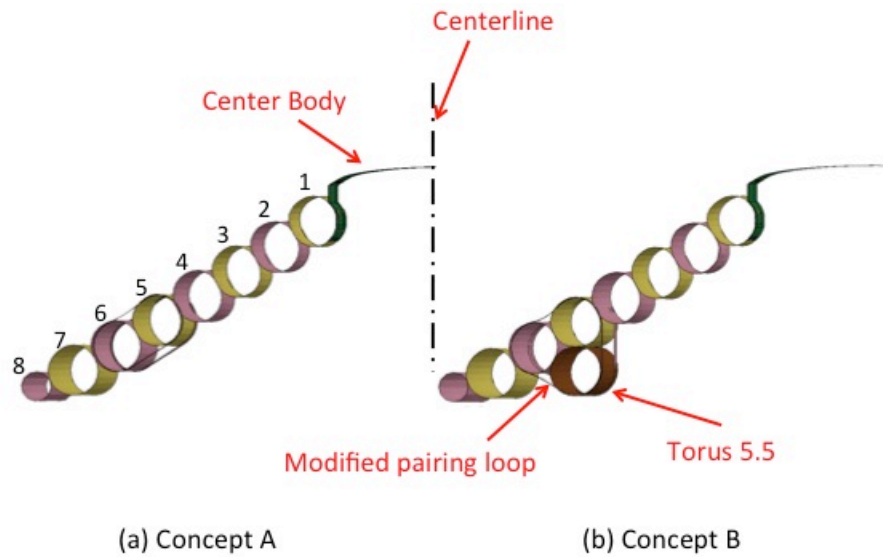


Figure 4. Cross-sectional illustration highlighting modifications to incorporate Torus 5.5 in Concept B.

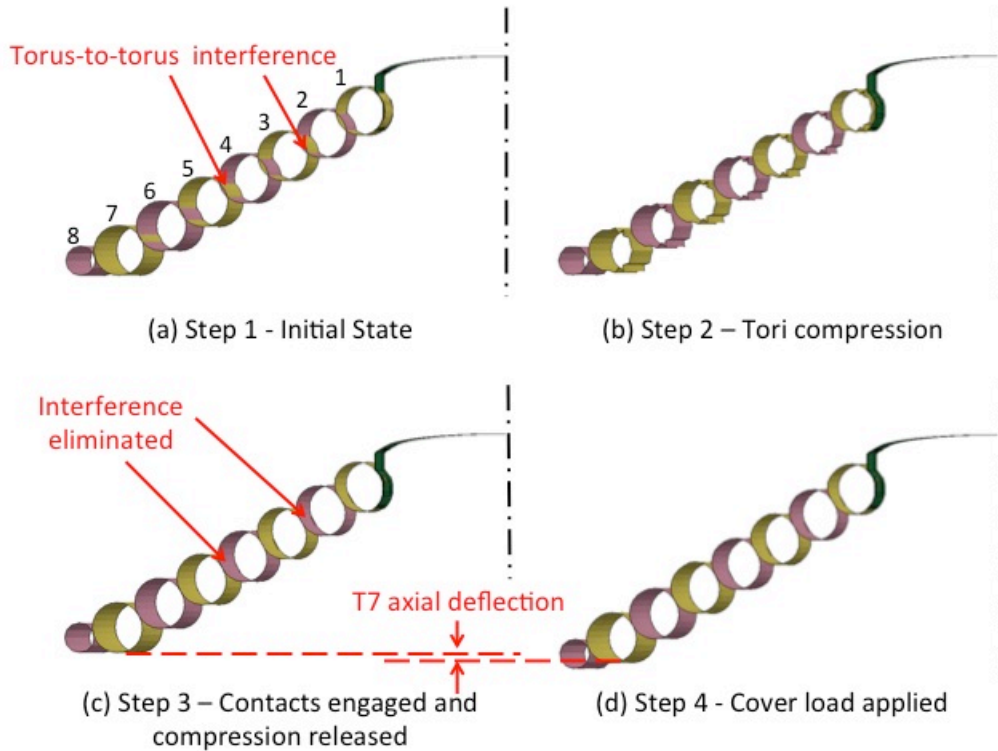


Figure 5. Nominal FEM loading states for HIAD simulations (cross-sectional view of Concept A).

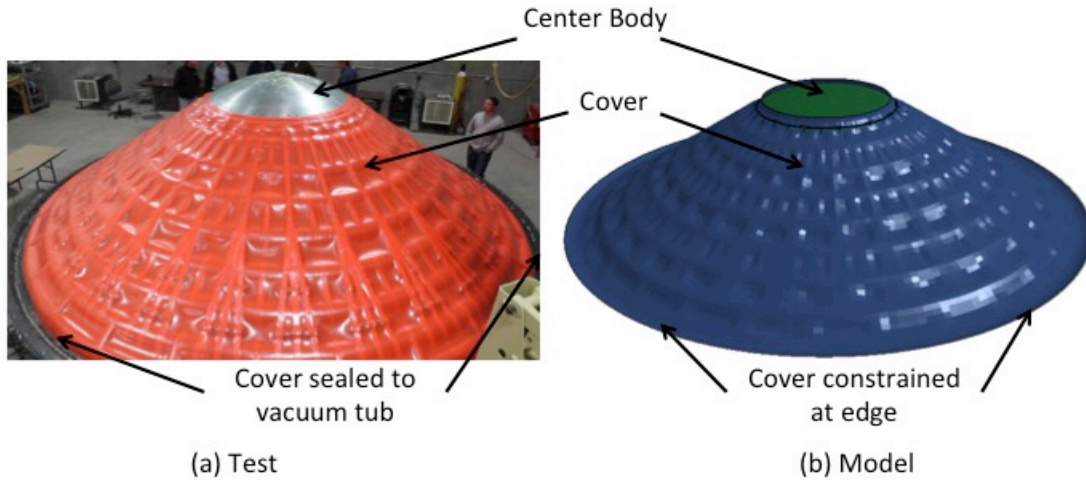


Figure 6. Representative test and analysis cover behavior at final loaded state.

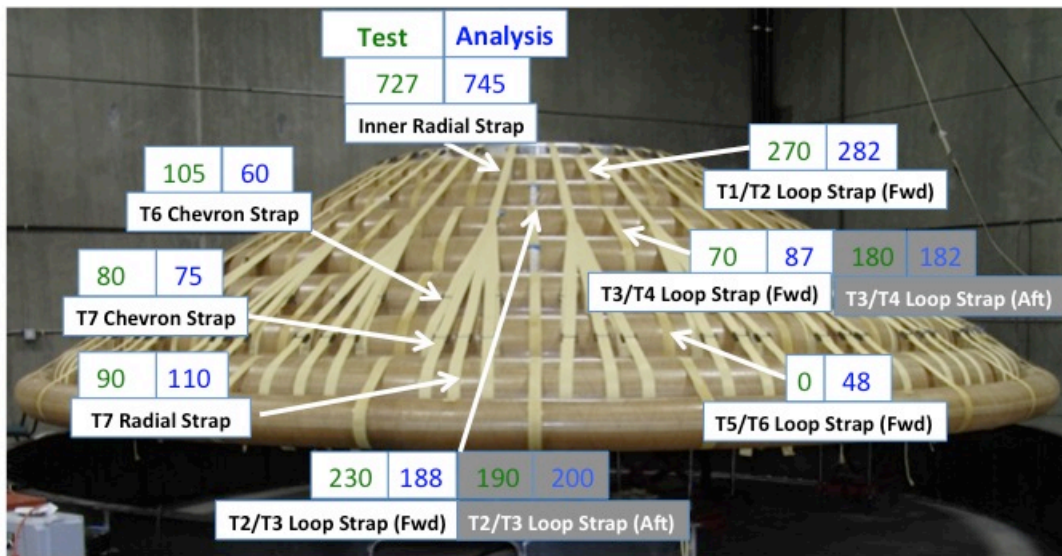


Figure 7. Comparison of strap load distribution for Concept A ($p_t=15\text{psi}$; $p_v=0.75\text{psi}$)

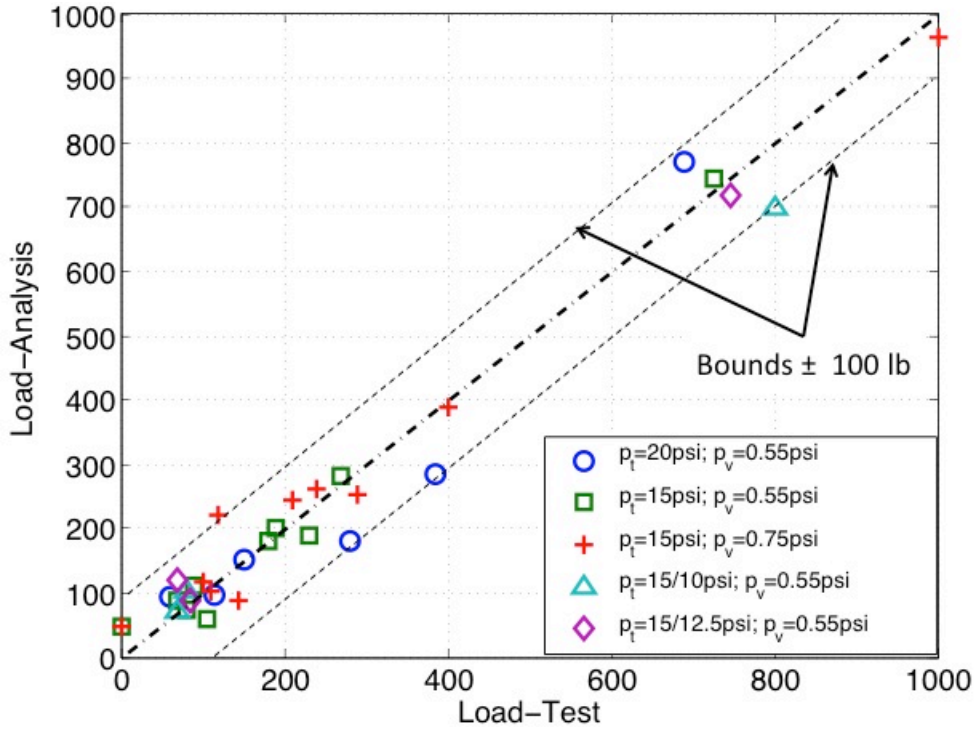


Figure 8. Comparison of test vs analysis for strap loads, Concept A.

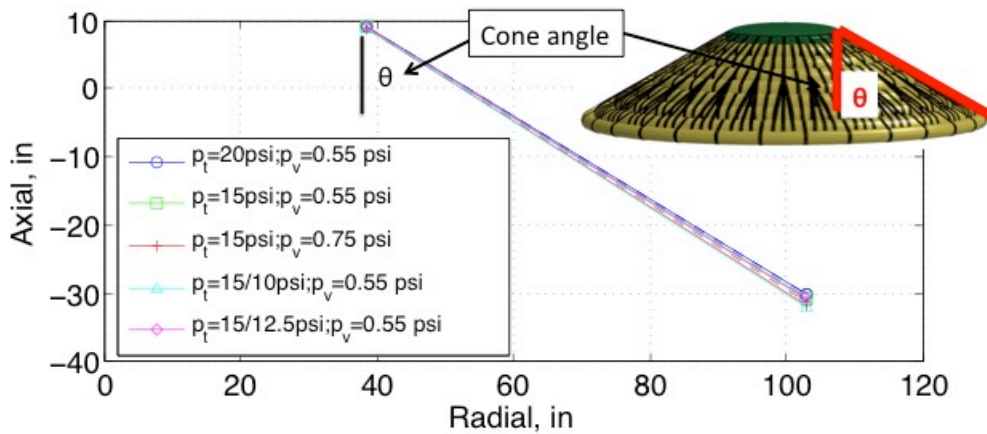


Figure 9. Comparison of test vs analysis for cone angle, Concept A. (Solid lines connect test data and dashed lines connect analysis.)

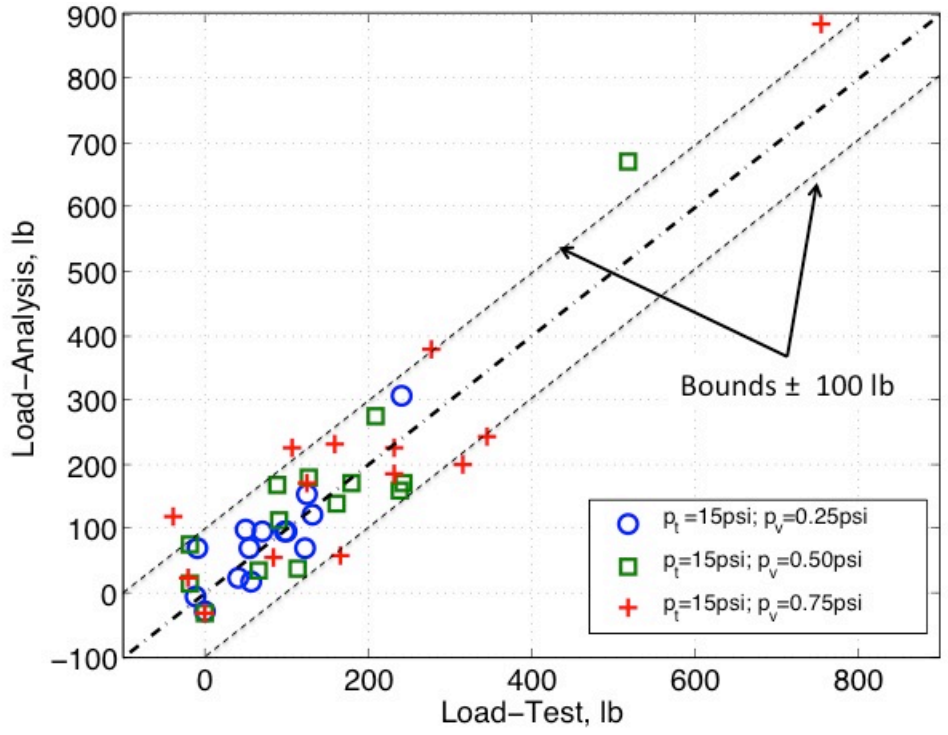


Figure 10. Comparison of test vs analysis for strap loads, Concept B.

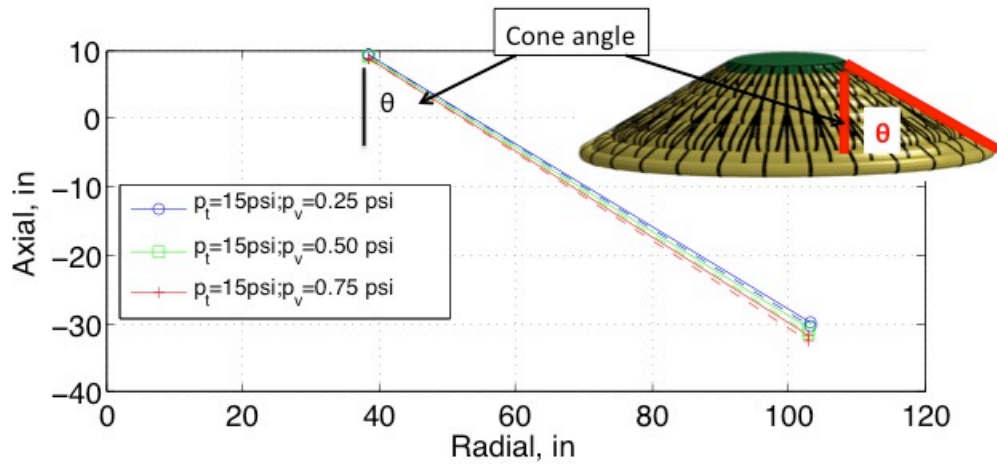


Figure 11. Comparison of test vs analysis for cone angle, Concept B. (Solid lines connect test data and dashed lines connect analysis.)

REPORT DOCUMENTATION PAGE

*Form Approved
OMB No. 0704-0188*

The public reporting burden for this collection of information is estimated to average 1 hour per response, including the time for reviewing instructions, searching existing data sources, gathering and maintaining the data needed, and completing and reviewing the collection of information. Send comments regarding this burden estimate or any other aspect of this collection of information, including suggestions for reducing this burden, to Department of Defense, Washington Headquarters Services, Directorate for Information Operations and Reports (0704-0188), 1215 Jefferson Davis Highway, Suite 1204, Arlington, VA 22202-4302. Respondents should be aware that notwithstanding any other provision of law, no person shall be subject to any penalty for failing to comply with a collection of information if it does not display a currently valid OMB control number.
PLEASE DO NOT RETURN YOUR FORM TO THE ABOVE ADDRESS.

1. REPORT DATE (DD-MM-YYYY) 01-07-2015		2. REPORT TYPE Technical Memorandum		3. DATES COVERED (From - To)	
4. TITLE AND SUBTITLE Comparison of Analysis with Test for Static Loading of Two Hypersonic Inflatable Aerodynamic Decelerator Concepts				5a. CONTRACT NUMBER	
				5b. GRANT NUMBER	
				5c. PROGRAM ELEMENT NUMBER	
6. AUTHOR(S) Lyle, Karen H.				5d. PROJECT NUMBER	
				5e. TASK NUMBER	
				5f. WORK UNIT NUMBER 77714.04.02.0	
7. PERFORMING ORGANIZATION NAME(S) AND ADDRESS(ES) NASA Langley Research Center Hampton, VA 23681-2199				8. PERFORMING ORGANIZATION REPORT NUMBER L-20573	
9. SPONSORING/MONITORING AGENCY NAME(S) AND ADDRESS(ES) National Aeronautics and Space Administration Washington, DC 20546-0001				10. SPONSOR/MONITOR'S ACRONYM(S) NASA	
				11. SPONSOR/MONITOR'S REPORT NUMBER(S) NASA-TM-2015-218778	
12. DISTRIBUTION/AVAILABILITY STATEMENT Unclassified - Unlimited Subject Category 18 Availability: NASA STI Program (757) 864-9658					
13. SUPPLEMENTARY NOTES					
14. ABSTRACT Acceptance of new spacecraft structural architectures and concepts requires validated design methods to minimize the expense involved with technology demonstration via flight-testing. Hypersonic Inflatable Aerodynamic Decelerator (HIAD) architectures are attractive for spacecraft deceleration because they are lightweight, store compactly, and utilize the atmosphere to decelerate a spacecraft during entry. However, designers are hesitant to include these inflatable approaches for large payloads or spacecraft because of the lack of flight validation. This publication summarizes results comparing analytical results with test data for two concepts subjected to representative entry, static loading. The level of agreement and ability to predict the load distribution is considered sufficient to enable analytical predictions to be used in the design process.					
15. SUBJECT TERMS Aerodynamic decelerator; Model correlation; Numerical analysis					
16. SECURITY CLASSIFICATION OF:			17. LIMITATION OF ABSTRACT	18. NUMBER OF PAGES	19a. NAME OF RESPONSIBLE PERSON
a. REPORT	b. ABSTRACT	c. THIS PAGE			STI Help Desk (email: help@sti.nasa.gov)
U	U	U	UU	19	19b. TELEPHONE NUMBER (Include area code) (757) 864-9658